

Research Article

Effect of Substrate Temperature on the Thermoelectric Properties of the Sb_2Te_3 Thin Films Deposition by Using Thermal Evaporation Method

Jyun-Min Lin,¹ Ying-Chung Chen,¹ Cheng-Fu Yang,² and Wei Chen¹

¹Department of Electrical Engineering, National Sun Yat-Sen University, Kaohsiung 804, Taiwan

²Department of Chemical and Materials Engineering, National University of Kaohsiung, Kaohsiung 811, Taiwan

Correspondence should be addressed to Cheng-Fu Yang; cfyang@nuk.edu.tw

Received 13 August 2014; Revised 15 October 2014; Accepted 15 October 2014

Academic Editor: Teen-Hang Meen

Copyright © 2015 Jyun-Min Lin et al. This is an open access article distributed under the Creative Commons Attribution License, which permits unrestricted use, distribution, and reproduction in any medium, provided the original work is properly cited.

The antimony-telluride (Sb_2Te_3) thermoelectric thin films were prepared on SiO_2/Si substrates by thermal evaporation method. The substrate temperature that ranged from room temperature to 150°C was adopted to deposit the Sb_2Te_3 thin films. The effects of substrate temperature on the microstructures and thermoelectric properties of the Sb_2Te_3 thin films were investigated. The crystal structure and surface morphology of the Sb_2Te_3 thin films were characterized by X-ray diffraction analyses and field emission scanning electron microscope observation. The RT-deposited Sb_2Te_3 thin films showed the amorphous phase. Te and Sb_2Te_3 phases were coexisted in the Sb_2Te_3 -based thin films as the substrate temperature was higher than room temperature. The average grain sizes of the Sb_2Te_3 -based thin films were 39 nm, 45 nm, 62 nm, 84 nm, and 108 nm, as the substrate temperatures were 50°C , 75°C , 100°C , 125°C , and 150°C , respectively. The Seebeck coefficients, electrical conductivity, and power factor were measured at room temperature; we had found that they were critically dependent on the substrate temperature.

1. Introduction

Facing the impact of the energy shortage and global warming problem, much attention to the issues of energy saving and reduction of carbon emission has been paid. The green technology is getting more and more attention, of which thermoelectric (TE) effect is one of the simplest technologies to convert energy by temperature difference and has recently attracted much attention. Thermoelectric materials can directly convert electricity from heat and vice versa. Hence, the application of thermoelectric materials is very promising for power generator and cooler [1, 2]. The energy conversion efficiency of the thermoelectric materials is judged by the figure of merit ZT , $ZT = (S^2\sigma/\kappa)T$, where T is defined as absolute temperature and S , σ , and κ are defined as Seebeck coefficient ($\Delta V/\Delta T$), electrical conductivity, and thermal conductivity, respectively [3, 4]. For that, the characteristics of TE materials depend on their S , σ , and κ , and the $S^2\sigma$ is defined as the power factor (PF). According to the

formula, the enhancement of thermoelectric figure of merit ZT can be obtained by raising the $S^2\sigma$ and the decrease of the thermal conductivity. Till now, the bismuth telluride- (Bi-Te-) and antimony-telluride- (Sb-Te-) based compounds are known to be the state-of-the-art thermoelectric materials for the applications near room temperature region. Furthermore, the Bi-Te- and Sb-Te-based thermoelectric materials show the highest figure of merit ZT and can be extensively utilized for the commercially available thermoelectric generators and coolers. For that, the Sb_2Te_3 alloy was used as the compound to investigate its thermoelectric characteristics.

Currently, the thermoelectric devices are manufactured by sintering blocks of the materials. So far, the thermoelectric materials used in applications have all been in bulk (3D), thin film (2D), and nanowire (1D) forms. However, the figure of merit (ZT) is low for the bulk materials. In order to improve the thermoelectric performance, the low-dimensional thermoelectric materials have been researched. Hicks and Dresselhaus had pointed out that low-dimensional

materials have better efficiency than bulk ones due to low-dimensional effects on both charge carriers and lattice waves [5]. Through the low-dimensional nanostructure, the thermoelectric materials can increase their density of states of Fermi level and enhance the phonon scattering of the materials [5]. However, it is difficult to miniaturize the thermoelectric devices by sintering blocks. Therefore, various deposition techniques have been proposed to obtain the thermoelectric thin films, such as flash evaporation [6, 7], ion-beam sputtering [8, 9], pulse laser deposition (PLD) [10, 11], sputtering [12, 13], electrochemical deposition [14, 15], metal organic chemical vapor deposition (MOCVD) [16, 17], and molecular beam epitaxy (MBE) [18, 19]. The electrochemical deposition was also a useful method to deposit thermoelectric materials in different morphologies, including thin films and nanowires [20, 21]. However, some processes need long time and expensive facilities to prepare the materials. In this paper, the thermal evaporation method is adopted to prepare Sb_2Te_3 thin films, because it is an attractive technology and offers some advantages, such as lower fabricating expenses and short processing time. In this work, the influence of substrate temperature on the microstructures and thermoelectric properties of the thermal evaporated thin films on silicon substrates was investigated.

2. Experimental

The p-type (1 0 0) silicon (Si) substrates were cleaned with standard RCA cleaning processes to remove the native oxide and particles. After that, a 400 nm thermally grown silicon dioxide (SiO_2) layer was deposited on the Si substrate by atmospheric pressure chemical vapor deposition (APCVD) method. Then, the thermoelectric thin films were deposited on SiO_2/Si substrates by the thermal evaporation method. The high-purity (99.99%) Sb_2Te_3 powder was used as evaporation source and evaporated from a tungsten boat. The size of the powders was in the range of 1 mm–10 mm, which was obtained by smashing the Sb_2Te_3 ingot. During the deposition process, a 60 A current was applied to the tungsten boat to evaporate the Sb_2Te_3 powder. The deposition rate of the Sb_2Te_3 thin films was estimated to be 16 Å/s. In this study, the thermoelectric thin films were prepared at the substrate temperature that ranged from room temperature to 150°C with chamber pressure of about 3.75×10^{-5} torr. As we know, the substrate temperature is the most important factor to affect the characteristics of the Sb_2Te_3 thin films, including thickness, crystalline structure, grain size, and pore ratio. For that, the substrate temperature will be the most important factor to affect the electrical characteristics of the Sb_2Te_3 thin films. As the substrate temperature was higher than 150°C, the Sb_2Te_3 thin films were hard to deposit on the Si substrates, for the fact that the substrate temperature was ranged from room temperature to 150°C. The thickness of the Sb_2Te_3 thin films was approximately 0.4 μm , independent of the substrate temperature.

The surface morphologies, deposition rate, and the thickness of thermoelectric thin films were observed by scanning electron microscopy (FE-SEM, JEOL JSM6700) with an

accelerating voltage of 10 kV. The crystalline structures of the thermoelectric thin films were determined by means of X-ray diffraction (XRD) (Cu-K α , Bruker D8). The diffraction angles (2θ) of thermoelectric Sb_2Te_3 thin films were revealed by scanning between 20° and 60° at the speed of 0.05° per second. For the investigation of thermoelectric properties, Seebeck coefficient (S) and electrical conductivity (σ) were measured at the room temperature. The Seebeck coefficient could be obtained by measuring the resulted Seebeck voltage as applying a temperature gradient across the sample, in which, the data was acquired by a Keithley 2700 system. As measured temperature was changed in a small range, for example, approximately 5°C, the Seebeck coefficient of the device under test (DUT) could be considered as a fixed value. Because the output voltage was not a steady value within the measuring time, the calculated Seebeck coefficient comprising the measured temperature gradient and output voltage could nearly be the constant values. During the measurement process, we used 10 seconds as the measurement time and ten Seebeck coefficient values could be obtained. Then, the average value of the ten data was taken as Seebeck coefficient value. The electrical conductivity of the specimens was measured by a conventional four-point probe method at room temperature. From S and σ , the thermoelectric power factor ($S^2\sigma$) was obtained.

3. Results and Discussion

Figure 1 shows the X-ray diffraction patterns of the standard Sb_2Te_3 alloy from the JCPD card and the raw Sb_2Te_3 alloy powder. The XRD diffraction peaks of the raw alloy powder were coincided with those of JCPDS card for Sb_2Te_3 alloy. This result indicates that the used alloy material for evaporation was single phase Sb_2Te_3 compound. For the raw Sb_2Te_3 alloy powder, four major diffraction peaks of 28.24°, 38.29°, 42.35°, and 44.58°, which are corresponding to (0 1 5), (1 0 10), (1 1 0), and (0 0 15) diffraction planes, were observed in Figure 1. Meanwhile, the raw Sb_2Te_3 alloy powder shows a preferred orientation corresponding to the (0 1 5) diffraction plane.

Figure 2 shows the X-ray diffraction patterns of the Sb_2Te_3 thin films deposited at various substrate temperatures. The crystalline properties of the Sb_2Te_3 thin films are apparently affected by the substrate temperature. The diffraction peaks in Figure 2 show that as the substrate temperature was changed; different alloy compounds were deposited during the evaporation process. As room temperature (RT) was used to deposit thin films, only the amorphous phase was observed. The reason is that the atoms did not have enough energy to proliferate and cluster on the substrate at room temperature. As the substrate temperature was higher than RT, the Te ((1 0 1) and (0 1 2)) and Sb_2Te_3 ((0 1 5), (1 0 10), (1 1 0), and (0 0 15)) phases were really observed in the XRD patterns. As the substrate temperature was increased from 50°C to 100°C, the diffraction intensities of the Te and Sb_2Te_3 phases increased with substrate temperature, showing that the crystallinity of the thin films was improved.

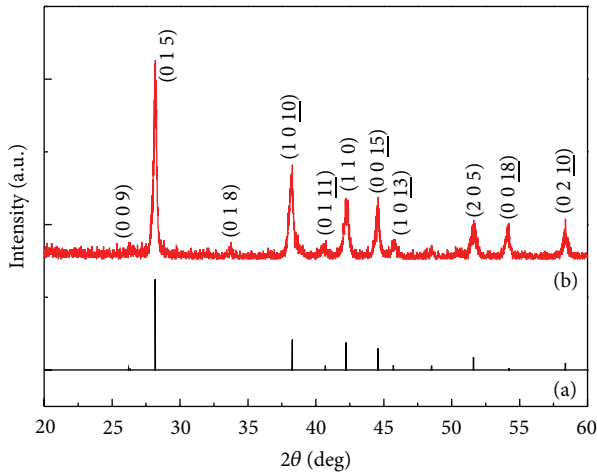


FIGURE 1: XRD patterns of (a) JCPDS card for Sb_2Te_3 material and (b) raw Sb_2Te_3 alloy powder.

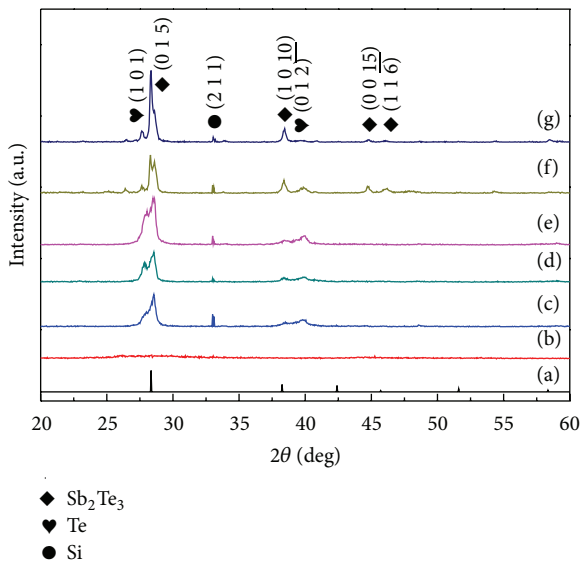


FIGURE 2: XRD patterns of the Sb_2Te_3 thin films deposited on SiO_2/Si substrates at various substrate temperatures: (a) JCPDS card, (b) room temperature, (c) 50°C , (d) 75°C , (e) 100°C , (f) 125°C , and (g) 150°C , respectively.

As 125°C was used as substrate temperature, the diffraction intensity of Te phase critically decreased and (0 1 5) plane of Sb_2Te_3 phase showed a splitting peak; as 150°C was used as substrate temperature, the diffraction intensity of (0 1 5) plane of Sb_2Te_3 phase critically increased and the full width at half maximum (FWHM) value of (0 1 5) plane decreased and a preferred orientation of (0 1 5) existed. The FWHM values of (0 1 5) plane were 0.525° , 0.512° , 0.478° , 0.385° , and 0.298° as the substrate temperatures were 50°C , 75°C , 100°C , 125°C , and 150°C , respectively. However, as the substrate temperature was higher than 150°C , the raw Sb_2Te_3 material was hard to deposit on the SiO_2/Si substrates. In this study, the optimum Sb_2Te_3 (0 1 5) plane of thin films was obtained at the substrate temperature of 150°C . The XRD

patterns shown in Figure 2 also suggest that the substrate temperature had large effect on the characteristics of the deposited Sb_2Te_3 thin films.

The SEM top-viewed images of the Sb_2Te_3 thin films deposited at various substrate temperatures are shown in Figure 3. As R.T. was used as substrate temperature, a continuous and smooth surface morphology was obtained; the deposited thin films with amorphous phase are the reason to cause this result. The figure also shows that as the substrate temperature was raised, the grain sizes increased with increasing substrate temperature. The average grain sizes were 39 nm, 45 nm, 62 nm, 84 nm, and 108 nm, as the substrate temperature was 50°C , 75°C , 100°C , 125°C , and 150°C , respectively. Those results prove that the polycrystalline structure, as XRD patterns in Figure 2 show, was obtained as the substrate temperature was equal to and higher than 50°C . Figure 4 shows the SEM cross-sectional microstructures of the deposited Sb_2Te_3 thin films under various substrate temperatures. As the substrate temperature was changed from R.T. to 100°C , the cross-sections of the deposited Sb_2Te_3 thin films showed a flat morphology and their thickness was around 400 nm; as the substrate temperature was higher than 100°C , the thickness was decreased and the size of pores increased with increasing substrate temperature. The increase in the size of pores is caused by the fact that the large grains grow at the expense of small ones, which result in the formation of new and larger voids where the small grains are originally located. As Figure 4 shows, the pores mainly grow in the vertical direction of the Sb_2Te_3 thin films as higher substrate temperature is used. As we know, the main composition of pores is air, which has very low conductivity. For that, even the electrical conductivity characteristic is mainly determined by the lateral structure of the Sb_2Te_3 thin films, the decrease in the conductivity of the Sb_2Te_3 thin films with increasing in the size of pores is expectable.

Figure 5 shows the variations of the electrical conductivity with various substrate temperatures. As the substrate temperature increased, the electrical conductivity of the deposited Sb_2Te_3 thin films first increased, reached a maximum at 100°C , and then decreased. The lower electrical conductivity of the RT-deposited thin films could be attributed to the poor crystallization, as confirmed by XRD analysis in Figure 2 and SEM surface observation in Figure 3. The electrical conductivity increased from $2.14 \times 10^2 \text{ S/cm}$ to $6.81 \times 10^2 \text{ S/cm}$ as the substrate temperature increased from R.T. to 100°C . With an increased substrate temperature from 100°C to 150°C , the electrical conductivity decreased from 6.81×10^2 to $3.11 \times 10^2 \text{ S/cm}$. The electrical conductivity of the Sb_2Te_3 thin films was enhanced as the substrate temperature is higher than RT. The improvement in the crystallization, as proven by XRD analysis in Figure 2 and SEM surface observation in Figure 3, is believed as the reason. As the substrate temperature is higher than 100°C , the pores increased with increasing temperature. Also, this is the reason to cause the decrease in conductivity.

Figure 6 shows the variation of the Seebeck coefficient with different substrate temperature. The results show that all samples have a positive Seebeck coefficient, which means that

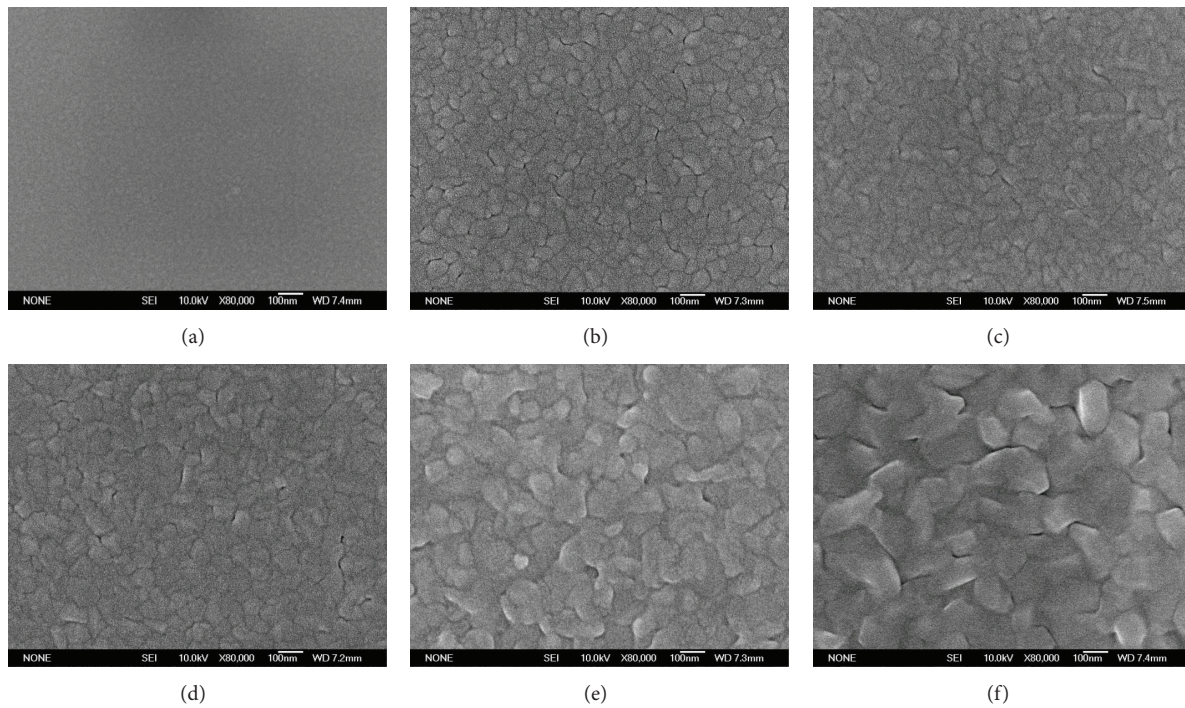


FIGURE 3: FE-SEM top-viewed morphologies of the Sb_2Te_3 thin films deposited under various substrate temperatures: (a) room temperature, (b) 50°C, (c) 75°C, (d) 100°C, (e) 125°C, and (f) 150°C, respectively.

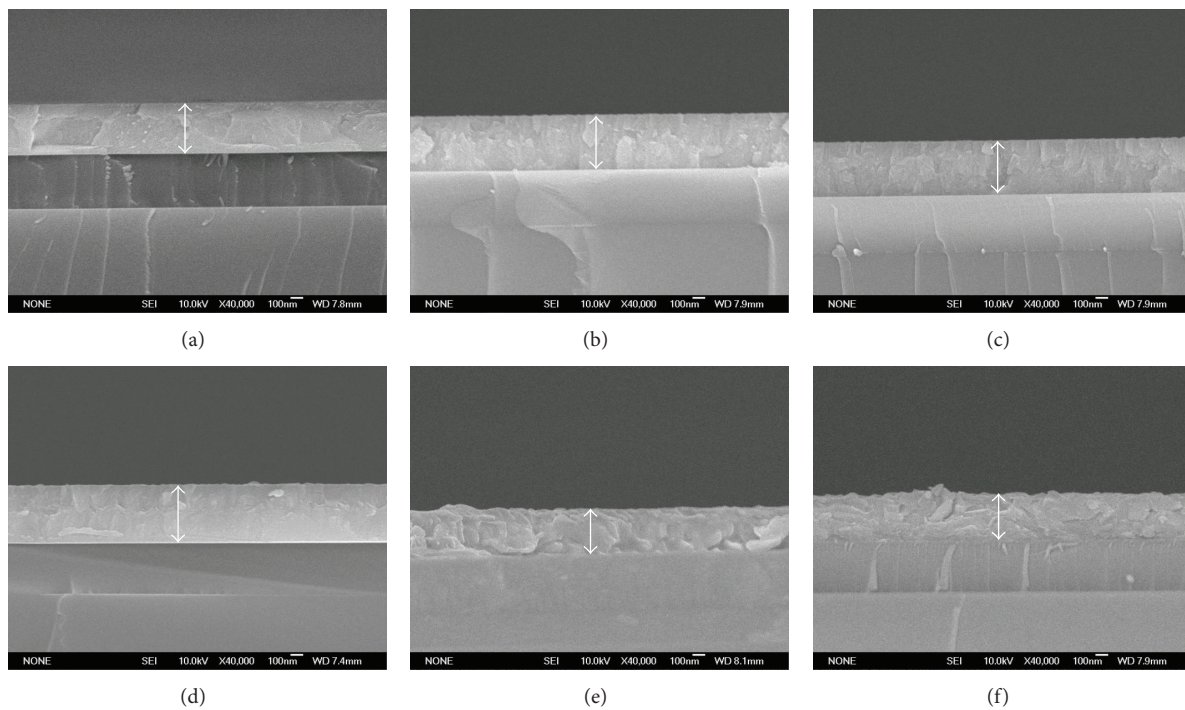


FIGURE 4: FE-SEM cross-sectional morphologies of the Sb_2Te_3 thin films deposited under various substrate temperatures: (a) room temperature, (b) 50°C, (c) 75°C, (d) 100°C, (e) 125°C, and (f) 150°C, respectively.

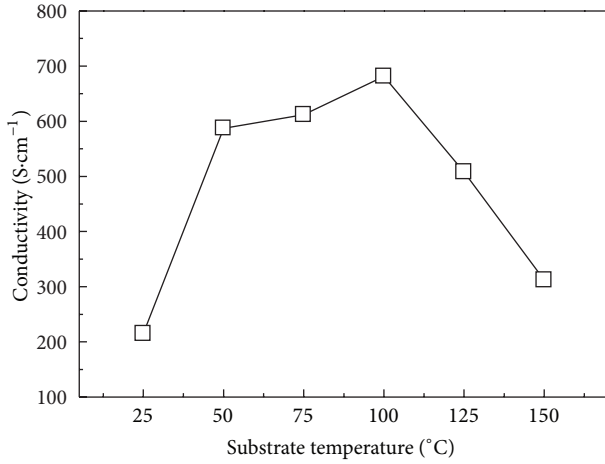


FIGURE 5: Variations of electrical conductivity for Sb_2Te_3 thin films deposited at various substrate temperatures.

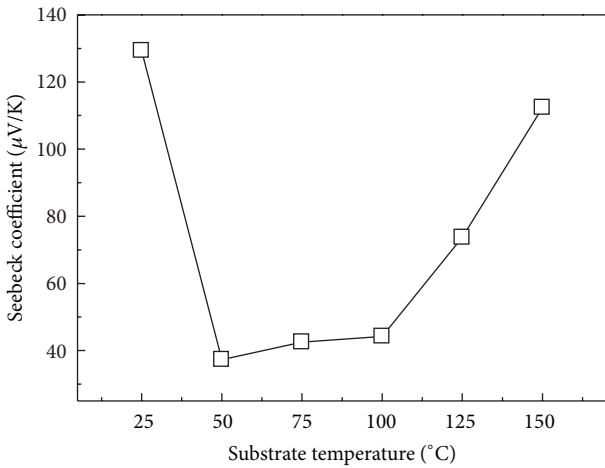


FIGURE 6: Variations of Seebeck coefficient for Sb_2Te_3 thin films deposited at various substrate temperatures.

the Sb_2Te_3 thin films are p-type semiconductors. According to the results, the samples deposited at R.T. show a large Seebeck coefficient ($\sim 129.3 \mu\text{V/K}$). The Seebeck coefficient decreased from $129.3 \mu\text{V/K}$ to $37.3 \mu\text{V/K}$ as the substrate temperature varied from R.T. to 50°C . After that, the Seebeck coefficient was enhanced as the substrate temperature increased from 50 to 150°C . The sample deposited at 150°C exhibited the large Seebeck coefficient of $112.4 \mu\text{V/K}$. It is well known that the Seebeck coefficient is closely related to the carrier concentration. In the case of p-type semiconductor crystals obeying Boltzmann statistics, the Seebeck coefficient (S) is given by the following equation [22]:

$$S = \pm \frac{k_B}{e} \left((\gamma + 2) + \ln \frac{2(2\pi m^* < k_B T)^{3/2}}{h^3 n} \right), \quad (1)$$

$$\sigma = ne\mu, \quad (2)$$

where k_B is Boltzmann's constant, e is the electron charge, r is the scattering factor, m^* is effective mass, h is Planck's

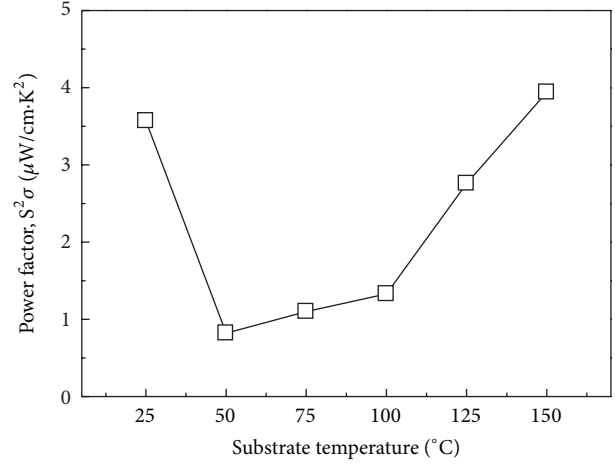


FIGURE 7: Variations of power factor for Sb_2Te_3 thin films deposited at various substrate temperatures.

constant, n is the carrier concentration, and μ is the carrier mobility, respectively. From (1), the Seebeck coefficient was found to be inversely proportional to the logarithmic scale of the carrier concentration. From (2) the conductivity is proportional to the carrier concentration, which may be caused by decreasing the number of defects. For that, the Seebeck coefficient of the thermoelectric thin films might be enhanced owing to the reduction of the conductivity. The results in Figures 5 and 6 prove that the Seebeck coefficient is inversely proportional to the electrical conductivity.

According to the results of Seebeck coefficient and electrical conductivity, the power factor can be calculated. The power factor is a significant thermoelectric parameter, which determines the performance of the thermoelectric converter. Figure 7 shows the power factors obtained for the Sb_2Te_3 thin films deposited at various substrate temperatures. Figure 7 shows that the power factor first drastically decreased as the substrate temperature increased from R.T. to 50°C ; then it increased as the substrate temperature was further increased from 50°C to 150°C . The thermoelectric properties for Sb_2Te_3 thin films deposited at various substrate temperatures are summarized in Table 1. Table 1 shows an important result that we can use the cheap evaporation equipment to deposit the Sb_2Te_3 thin films with high Seebeck coefficient and acceptable power factor. It also shows that the optimized Seebeck coefficient and power factor of the Sb_2Te_3 p-type thin films were found to be about $112.4 \mu\text{V/K}$ and $3.94 \mu\text{W/cm}\cdot\text{K}^2$ at the substrate temperature of 150°C , respectively.

4. Conclusion

In this study, a thermal evaporation method was successfully utilized for the deposition of the Sb_2Te_3 -based thermoelectric thin films from R.T. to 150°C on SiO_2/Si substrates with low-cost. We found that as the substrate temperature was higher than 150°C , the raw Sb_2Te_3 material was hard to deposit on the SiO_2/Si substrates. The electrical conductivity increased from $2.14 \times 10^2 \text{ S/cm}$ to $6.81 \times 10^2 \text{ S/cm}$ as the substrate

TABLE 1: Thermoelectric properties of the Sb_2Te_3 thin films deposited at various substrate temperatures.

Substrate temperature (°C)	Seebeck coefficient ($\mu\text{W/K}$)	Conductivity ($\text{S}\cdot\text{cm}^{-1}$)	Power factor ($\mu\text{W}/\text{cm}\cdot\text{K}^2$)
R.T.	129.3	214.75	3.57
50	37.3	587.30	0.80
75	42.5	611.80	1.10
100	44.2	681.57	1.33
125	73.7	508.20	2.76
150	112.4	311.99	3.94

temperature increased from R.T. to 100°C. With an increased substrate temperature from 100°C to 150°C, the electrical conductivity decreased from 6.81×10^2 to 3.11×10^2 S/cm. The Seebeck coefficient decreased from 129.3 $\mu\text{V/K}$ to 37.3 $\mu\text{V/K}$ as the substrate temperature varied from R.T. to 50°C. After that, the Seebeck coefficient was enhanced as the substrate temperature increased from 50 to 150°C. As the substrate temperature increased to 150°C, the Seebeck coefficient and power factor of p-type Sb_2Te_3 -based thin films were found to be about 112.4 $\mu\text{V/K}$ and 3.94 $\mu\text{W}/\text{cm}\cdot\text{K}^2$, respectively.

Conflict of Interests

The authors declare that there is no conflict of interests regarding the publication of this paper.

Acknowledgment

The authors gratefully acknowledge the financial support from the Contract of MOST 103-2221-E-110-075-MY2.

References

- [1] W. L. Luan and S. T. Tu, "Recent development of thermoelectric generation," *Chinese Science Bulletin*, vol. 49, pp. 1–8, 2004.
- [2] K. H. Lee and O. J. Kim, "Analysis on the cooling performance of the thermoelectric micro-cooler," *International Journal of Heat and Mass Transfer*, vol. 50, no. 9–10, pp. 1982–1992, 2007.
- [3] D. M. Rowe, *Thermoelectrics Handbook: Macro to Nano*, CRC & Taylor & Francis, Boca Raton, Fla, USA, 2006.
- [4] T. M. Tritt, "Holey and unholey semiconductors," *Science*, vol. 283, no. 5403, pp. 804–805, 1999.
- [5] L. D. Hicks and M. S. Dresselhaus, "Effect of quantum-well structures on the thermoelectric figure of merit," *Physical Review B*, vol. 47, no. 19, pp. 12727–12731, 1993.
- [6] A. Foucaran, A. Sackda, A. Giani, F. Pascal-Delannoy, and A. Boyer, "Flash evaporated layers of $(\text{Bi}_2\text{Te}_3\text{-Bi}_2\text{Se}_3)(\text{N})$ and $(\text{Bi}_2\text{Te}_3\text{-Sb}_2\text{Te}_3)(\text{P})$," *Materials Science and Engineering B*, vol. 52, no. 2–3, pp. 154–161, 1998.
- [7] M. Takashiri, T. Shirakawa, K. Miyazaki, and H. Tsukamoto, "Fabrication and characterization of bismuth-telluride-based alloy thin film thermoelectric generators by flash evaporation method," *Sensors and Actuators A*, vol. 138, no. 2, pp. 329–334, 2007.
- [8] H. Noro, K. Sato, and H. Kagechika, "The thermoelectric properties and crystallography of Bi-Sb-Te-Se thin films grown by ion beam sputtering," *Journal of Applied Physics*, vol. 73, no. 3, pp. 1252–1260, 1993.
- [9] P. Fan, Z. H. Zheng, G. X. Liang, D. P. Zhang, and X. M. Cai, "Thermoelectric characterization of ion beam sputtered Sb_2Te_3 thin films," *Journal of Alloys and Compounds*, vol. 505, no. 1, pp. 278–280, 2010.
- [10] R. S. Makala, K. Jagannadham, and B. C. Sales, "Pulsed laser deposition of Bi_2Te_3 -based thermoelectric thin films," *Journal of Applied Physics*, vol. 94, no. 6, pp. 3907–3918, 2003.
- [11] H. Obara, S. Higomo, M. Ohta, A. Yamamoto, K. Ueno, and T. Iida, "Thermoelectric properties of Bi_2Te_3 -based thin films with fine grains fabricated by pulsed laser deposition," *Japanese Journal of Applied Physics*, vol. 48, no. 8, Article ID 085506, 2009.
- [12] H. Huang, W.-L. Luan, and S.-T. Tu, "Influence of annealing on thermoelectric properties of bismuth telluride films grown via radio frequency magnetron sputtering," *Thin Solid Films*, vol. 517, no. 13, pp. 3731–3734, 2009.
- [13] B. Fang, Z. Zeng, X. Yan, and Z. Hu, "Effects of annealing on thermoelectric properties of Sb_2Te_3 thin films prepared by radio frequency magnetron sputtering," *Journal of Materials Science: Materials in Electronics*, vol. 24, no. 4, pp. 1105–1111, 2013.
- [14] F. Xiao, C. Hangarter, B. Yoo, Y. Rheem, K.-H. Lee, and N. V. Myung, "Recent progress in electrodeposition of thermoelectric thin films and nanostructures," *Electrochimica Acta*, vol. 53, no. 28, pp. 8103–8117, 2008.
- [15] Y. Ma, E. Ahlberg, Y. Sun, B. B. Iversen, and A. E. C. Palmqvist, "Thermoelectric characteristics of electrochemically deposited Bi_2Te_3 and Sb_2Te_3 thin films of relevance to multilayer preparation," *Journal of the Electrochemical Society*, vol. 159, no. 2, pp. D50–D58, 2012.
- [16] A. Giani, A. Boulouz, F. Pascal-Delannoy, A. Foucaran, E. Charles, and A. Boyer, "Growth of Bi_2Te_3 and Sb_2Te_3 thin films by MOCVD," *Materials Science and Engineering B: Solid-State Materials for Advanced Technology*, vol. 64, no. 1, pp. 19–24, 1999.
- [17] A. Giani, A. Boulouz, F. Pascal-Delannoy et al., "Electrical and thermoelectrical properties of Sb_2Te_3 prepared by the metal-organic chemical vapor deposition technique," *Journal of Materials Science Letters*, vol. 18, no. 7, pp. 541–543, 1999.
- [18] H. Cao, R. Venkatasubramanian, C. Liu et al., "Topological insulator Bi_2Te_3 films synthesized by metal organic chemical vapor deposition," *Applied Physics Letters*, vol. 101, no. 16, Article ID 162104, 2012.
- [19] Y. Kim, A. Divenere, G. K. L. Wong, J. B. Ketterson, S. Cho, and J. R. Meyer, "Structural and thermoelectric transport properties of Sb_2Te_3 thin films grown by molecular beam epitaxy," *Journal of Applied Physics*, vol. 91, no. 2, pp. 715–718, 2002.
- [20] Y. Jia, D. Yang, B. Luo, S. Liu, M. O. Tade, and L. Zhi, "One-pot synthesis of Bi-Ni nanowire and nanocable arrays by coelectrodeposition approach," *Nanoscale Research Letters*, vol. 7, article 130, 2012.
- [21] C.-G. Kuo, Y.-T. Hsieh, C.-F. Yang, C.-H. Huang, and C.-Y. Yen, "Growth of anodic aluminum oxide templates and the application in fabrication of the BiSbTe-based thermoelectric nanowires," *International Journal of Photoenergy*, vol. 2014, Article ID 978184, 7 pages, 2014.
- [22] G. S. Nolas, J. Sharp, and H. J. Goldsmid, *Thermoelectrics: Basic Principles and New Materials Developments*, Springer, Berlin, Germany, 2001.



Hindawi

Submit your manuscripts at
<http://www.hindawi.com>

